



HAL
open science

Loss of endothelial sulfatase-1 after experimental sepsis attenuates subsequent pulmonary inflammatory responses

Kaori Oshima, Xiaorui Han, Yilan Ouyang, Rana El Masri, Yimu Yang, Sarah Haeger, Sarah Mcmurtry, Trevor Lane, Pavel Davizon-Castillo, Fuming Zhang, et al.

► To cite this version:

Kaori Oshima, Xiaorui Han, Yilan Ouyang, Rana El Masri, Yimu Yang, et al.. Loss of endothelial sulfatase-1 after experimental sepsis attenuates subsequent pulmonary inflammatory responses. *American Journal of Physiology - Lung Cellular and Molecular Physiology*, 2019, 10.1152/ajplung.00175.2019 . hal-02279983

HAL Id: hal-02279983

<https://hal.science/hal-02279983>

Submitted on 5 Jan 2021

HAL is a multi-disciplinary open access archive for the deposit and dissemination of scientific research documents, whether they are published or not. The documents may come from teaching and research institutions in France or abroad, or from public or private research centers.

L'archive ouverte pluridisciplinaire **HAL**, est destinée au dépôt et à la diffusion de documents scientifiques de niveau recherche, publiés ou non, émanant des établissements d'enseignement et de recherche français ou étrangers, des laboratoires publics ou privés.

1 **Title:** Loss of endothelial sulfatase-1 after experimental sepsis attenuates subsequent
2 pulmonary inflammatory responses

3 **Abbreviated title:** Endothelial loss of Sulf-1 and post-septic CARS

4 **Authors:** Kaori Oshima¹, Xiaorui Han², Yilan Ouyang², Rana El Masri³, Yimu Yang¹,
5 Sarah M. Haeger¹, Sarah A. McMurtry¹, Trevor C. Lane¹, Pavel Davizon-Castillo^{4,5},
6 Fuming Zhang², Xinping Yue⁶, Romain R. Vivès³, Robert J. Linhardt², Eric P. Schmidt^{1,7}

7

8 **Author affiliations:**

9 ¹Department of Medicine, University of Colorado Denver, Aurora, Colorado, USA

10 ²Departments of Chemistry and Chemical Biology, Chemical and Biological Engineering,
11 and Biomedical Engineering, Rensselaer Polytechnic Institute, Troy, New York, USA

12 ³University of Grenoble Alpes, CNRS, CEA, IBS, Grenoble, France

13 ⁴Department of Pediatrics, University of Colorado Denver, Aurora, Colorado, USA

14 ⁵Hemophilia and Thrombosis Center, School of Medicine, University of Colorado,
15 Aurora, CO, USA

16 ⁶Department of Physiology School of Medicine, Louisiana State University Health
17 Sciences Center, New Orleans, Louisiana, USA

18 ⁷Department of Medicine, Denver Health Medical Center, Denver, Colorado, USA

19

20 **Corresponding Author:**

21 Eric P. Schmidt, MD

22 12700 E. 19th Avenue, Research Complex 2, Mail Stop C272

23 Aurora CO, 80045.

24 Phone: (303) 724-6106

25 E-mail: eric.schmidt@ucdenver.edu

26

27

28 **Author Contributions:**

29 K.O. and E.P.S. conceived and designed the study; K.O., Y.Y., S.M.H., S.A.M., T.L.,
30 P.D-C, R.E.M. performed experiments; K.O., S.A.M, E.P.S. analyzed data; K.O., R.E.M.,
31 R.R.V., and E.P.S. prepared figures; K.O. and E.P.S. drafted manuscript; K.O., Y.Y.,
32 S.M.H., S.A.M., T.L., R.E.M., F.Z., X.Y., R.R.V., R.J.L., E.P.S. edited and revised
33 manuscript; K.O., Y.Y., S.M.H., S.A.M., T.L., R.E.M., F.Z., X.Y., R.R.V., R.J.L., E.P.S.
34 approved the final version of the manuscript.

35

36 **Keywords:**

37 Heparan sulfate, Sulfatase-1, Compensatory anti-inflammatory response syndrome

38 **Abstract**

39 Sepsis patients are at increased risk for hospital-acquired pulmonary infections,
40 potentially due to post-septic immunosuppression known as the compensatory anti-
41 inflammatory response syndrome (CARS). CARS has been attributed to leukocyte
42 dysfunction, with an unclear role for endothelial cells. The pulmonary circulation is lined
43 by an endothelial glycocalyx, a heparan sulfate-rich layer essential to pulmonary
44 homeostasis. Heparan sulfate degradation occurs early in sepsis, leading to lung injury.
45 Endothelial synthesis of new heparan sulfates subsequently allows for glycocalyx
46 reconstitution and endothelial recovery. We hypothesized that remodeling of the
47 reconstituted endothelial glycocalyx, mediated by alterations in the endothelial
48 machinery responsible for heparan sulfate synthesis, contributes to CARS. 72 hours
49 after experimental sepsis, coincident with glycocalyx reconstitution, mice demonstrated
50 impaired neutrophil and protein influx in response to intratracheal lipopolysaccharide
51 (LPS). The post-septic reconstituted glycocalyx was structurally remodeled, with
52 enrichment of heparan sulfate disaccharides sulfated at the 6-O position of glucosamine.
53 Increased 6-O-sulfation coincided with loss of endothelial sulfatase-1 (Sulf-1), an
54 enzyme that specifically removes 6-O-sulfates from heparan sulfate. Intravenous
55 administration of Sulf-1 to post-septic mice restored the pulmonary response to LPS,
56 suggesting that loss of Sulf-1 was necessary for post-septic suppression of pulmonary
57 inflammation. Endothelial-specific knockout mice demonstrated that loss of Sulf-1 was
58 not sufficient to induce immunosuppression in non-septic mice. Knockdown of Sulf-1 in
59 human pulmonary microvascular endothelial cells resulted in downregulation of the
60 adhesion molecule ICAM-1. Taken together, our study indicates that loss of endothelial

- 61 Sulf-1 is necessary for post-septic suppression of pulmonary inflammation, representing
62 a novel endothelial contributor to CARS.

63 **Introduction**

64 Sepsis, defined as life-threatening organ dysfunction caused by a dysregulated host
65 immune response (34), is a leading cause of in-hospital mortality worldwide (12).

66 Classically, septic organ injury has been attributed to systemic, overwhelming hyper-
67 inflammation. However, the failures of numerous clinical trials targeting inflammatory
68 signaling (18) led to the proposed concept that sepsis is not simply hyper-inflammation,
69 but also consists of a delayed period of immunosuppression, known as the
70 compensatory anti-inflammatory response syndrome (CARS) (1). This period of
71 suppressed inflammation is paradoxically harmful in sepsis, imparting an increased risk
72 for secondary infections (9, 15, 26, 35) such as hospital-acquired pneumonia (15, 39).
73 Evidence supporting the pathologic significance of post-septic CARS includes known
74 associations between mortality and increased plasma IL-10 and decreased HLA-DR
75 expression on leukocytes (10, 16, 21), decreased production of cytokines, such as
76 $TNF\alpha$, $IFN-\gamma$, IL-6, IL-10 in septic patients, and depletion of CD4+, CD8+, HLA-DR+
77 cells in the spleen (2). CARS has therefore been largely attributed to dysfunctional
78 monocytes, including impaired cytokine production, decreased phagocytosis and
79 migration in response to inflammatory stimuli (23, 44). Despite the potential importance
80 of CARS, clinical trials targeting immunosuppression have been disappointing (18, 19,
81 25), perhaps reflecting an incomplete understanding of the mechanisms responsible
82 post-septic impairment in lung inflammation.

83 The endothelial glycocalyx is carbohydrate-rich endovascular layer that serves multiple
84 homeostatic functions at the endothelial surface. The major glycosaminoglycan
85 constituent of the glycocalyx is heparan sulfate (HS), a linear polysaccharide composed

86 of repeating glucosamine and hexuronic (glucuronic and iduronic) acid disaccharide
87 units. This disaccharide unit may be sulfated at the amino (*N*) and/or 6-*O* positions of
88 glucosamine and/or the 2-*O* position of hexuronic acid. The resultant pattern of
89 negative charge enables HS to bind to various cationic ligands and their cognate
90 receptors (11, 28), influencing multiple signaling processes responsible for organ injury
91 and repair.

92 We have previously reported that sepsis-induced degradation of HS from the pulmonary
93 endothelial glycocalyx mediates alveolar neutrophil adhesion and inflammatory lung
94 injury (31). During sepsis recovery (72 hours after cecal ligation and puncture (CLP) in
95 mice), endothelial synthesis of new HS allows for glycocalyx reconstitution, mediating
96 endothelial recovery (45). We postulated that post-septic changes in the endothelial
97 machinery responsible for endothelial HS synthesis lead to remodeling of the
98 endothelial glycocalyx, impairing pulmonary responses to subsequent inflammatory
99 stimuli.

100 In this report, we observed that mice demonstrated suppressed pulmonary inflammation
101 in response to intratracheal lipopolysaccharides (LPS) after experimental sepsis,
102 coincident with glycocalyx enrichment in 6-*O*-sulfated HS, a sulfation pattern implicated
103 in endothelial inflammation (27, 41). This remodeling was associated with
104 downregulation of pulmonary endothelial Sulf-1, an enzyme responsible for the
105 constitutive cleavage of extracellular 6-*O*-sulfo groups. We observed that loss of Sulf-1
106 in septic mice was necessary for the impaired pulmonary response to LPS characteristic
107 of CARS, but it was not sufficient to cause impaired inflammation in non-septic animals.
108 Knock down of Sulf-1 using siRNA in pulmonary microvascular endothelial cells resulted

109 in downregulation of ICAM-1 transcription. Our study therefore identifies post-septic
110 remodeling of the pulmonary endothelial glycocalyx as a novel contributor to CARS.

111

112 **Materials and Method**

113

114 **Materials**

115 We purchased LPS (from *Escherichia coli* O55:B5), heparinase I and III (from
116 *Flavobacterium heparinum*) from Sigma-Aldrich (St. Louis, MO) and reconstituted in
117 phosphate buffered saline (PBS). As controls, we heat-inactivated heparinase I and III
118 at 100°C for 20 min. We purchased protein assay dye reagent from Bio-Rad (Hercules,
119 CA). We purchased tamoxifen from Sigma-Aldrich and dissolved in corn oil with 5%
120 ethanol. For tissue digestion and fluorescence activated cell sorting, we purchased
121 collagenase type 2 from Worthington Biochemical Corporation (Lakewood, NJ), dispase
122 I from Sigma-Aldrich, and ACK lysing buffer from Gibco (Dublin, Ireland). We
123 purchased anti-mouse CD31-APC antibody (17-0311-82, Clone:390) from eBioscience
124 (San Diego, CA), and anti-mouse CD144-PE antibody (562243, Clone: 11D4.1) from
125 BD Biosciences (San Jose, CA) and DAPI from Invitrogen (Carlsbad, CA). For
126 quantitative Reverse Transcription-Polymerase Chain Reaction (qRT-PCR), we
127 purchased reagents for RNA extraction and DNase I from Qiagen (Hilden, Germany).
128 We purchased primary human pulmonary microvascular endothelial cells from
129 PromoCell (Heidelberg, Germany). We purchased iScript cDNA synthesis kit from Bio-
130 Rad. We purchased siRNA targeted for sulfatase-1 (Sulf-1) from Dharmacon (Lafayette,
131 CO), and purchased transfection reagent, Lipofectamine RNAiMAX, from Thermo
132 Fisher Scientific (Waltham, MA). For production of recombinant HSulf-1, we purchased
133 all tissue culture reagents and media, from Thermo Fisher Scientific, and
134 chromatography reagents from GE Healthcare (Chicago, IL).

135

136 **Animals**

137 All experimental protocols were approved by the University of Colorado Institutional
138 Animal Care Use Committee, and all experiments were performed in accordance of
139 National Institutes of Health guideline. Wild type, male C57BL/6J mice (8-10 weeks)
140 were purchased from Jackson Laboratory. Sulf-1 and 2 double floxed mice (both males
141 and females, 8-12 weeks old) were used as previously described (37). VE-cadherin
142 CRE-ERT2 mice were provided by Dr. Ralf Adams at Max Planck Institute, Germany.
143 Sulf1/2 double homozygous mice with or without VE-cadherin-CRE-ERT2 (Sulf-1^{ff} Sulf-
144 2^{ff} VEcadCreERT2^{-or+}) were used for all knock out animal experiments. CRE-ERT2
145 translocation to nucleus was induced with intraperitoneal injections of tamoxifen
146 (dissolved in corn oil and 5% ethanol, sterile filtered), 1 mg/day, for 5 consecutive days.

147 **Induction of sepsis in mice**

148 We induced sepsis in 8-14 week-old mice with CLP as previously described (31).
149 Briefly, we anesthetized animals with 5% isoflurane inhalation. An incision of
150 approximately 1 cm was made in abdomen and cecum was exposed. We ligated the
151 cecum at 50 % of its length and punctured it through and through with a 22 G needle.
152 The cecum was then returned to the abdominal cavity, and the incision was closed with
153 suture. Buprenorphine (1.6 µg/ g body weight, i.p.) was given to each animal for pain
154 management, and 1 mL of sterile saline was given subcutaneously as fluid resuscitation.
155 Sham surgery was performed similarly, albeit without ligation and puncture of the cecum.

156 **Intratracheal instillation**

157 We anesthetized animals with 5 % isoflurane inhalation, and we instilled LPS at 3 μ g/g
158 body weight to trachea visualized with laryngoscope. Animals spontaneously breathed
159 throughout the instillation.

160 **Blood analysis**

161 We collected blood from the retro-orbital sinus using heparin-coated capillary tubes, and
162 determined complete blood counts (CBCs) using a veterinary hematology analyzer
163 (Heska, Loveland, CO). We collected blood anticoagulated with 3.8% citrate by cardiac
164 puncture and assessed global hemostasis using kaolin as activator by
165 thromboelastography (Haemonetics, BrainTree, MA).

166 **Tissue and sample collection**

167 We anesthetized mice with a lethal dose of ketamine/xylazine, and collected blood in
168 EDTA tubes by inferior vena cava cannulation. We collected plasma by centrifuging
169 whole blood at 1000 x g for 10 min. and stored it at -80 °C until analysis. We
170 cannulated the trachea and performed bronchoalveolar lavage (BAL) 3 times with 1 mL
171 of PBS each. We flushed blood out of the lung by pulmonary artery perfusion, and the
172 right lung was snap frozen with liquid N₂ and stored at -80 °C until analysis. We inflated
173 the left lung with 1% low-melting agarose in PBS, fixed with 10% formalin overnight, and
174 processed the tissue for histological analysis. We determined total cells per mL in BAL
175 fluid using a hemocytometer. We centrifuged BAL fluid at 1200 rpm for 5 min. and
176 stored the supernatant at -80 °C until analysis. We determined total protein
177 concentration in BAL fluid with a Coomassie Brilliant Blue-based colorimetric assay.

178 Cells in BAL fluid were mounted on a slide with cytospin at 600 rpm for 2 min., and
179 stained with Wright-Giemsa method for differential cell counting.

180 **Isolated perfused mouse lung**

181 We performed the isolated, perfused mouse lung as previously described (29). Briefly,
182 we deeply anesthetized mice with ketamine and xylazine. After confirming the loss of
183 toe-pinch reflex, we cannulated the trachea and ventilated mice with 21% O₂ and 5%
184 CO₂ at 125 breaths/min at tidal volume of 250 μ L. We rapidly removed the sternum and
185 anterior chest wall, and then cannulated the pulmonary artery through an incision made
186 in the free wall of the right ventricle. We cannulated the left atrium through an incision
187 made at the left ventricular apex. We secured the cannulas in position with suture. We
188 then perfused the pulmonary circulation with endothelial cell growth media
189 supplemented with 4% (g/mL) bovine serum albumin at 1 mL/min flow. Perfusate was
190 kept at 37°C with a water bath. We then added 0.5 unit/mL of heparinase I and III mix
191 to the perfusate and continued isogravimetric perfusion for 30 min. At the end of the
192 experiment, we collected perfusate and stored it at -80°C until mass spectrometric
193 analysis.

194 **Measurement of glycocalyx thickness with intravital microscopy**

195 We performed intravital microscopy as previously described (31). Briefly, we
196 anesthetized animals with ketamine and xylazine, and placed a glass window
197 (coverslip) into the right anterior thoracic wall. We infused 150 kDa FITC-dextran into
198 the jugular vein to serve as vascular tracer that does not penetrate the glycocalyx. We
199 injected either heparinase I or III and captured pulmonary microvasculature for 1.5 h.

200 We used a custom-designed intravital microscope (31) to simultaneously measure total
201 vessel width (endothelial cell border to the opposite endothelial cell border, as defined
202 by differential interference contrast microscopy) as well as FITC-dextran width (which
203 does not include the glycocalyx). We determined glycocalyx thickness by subtracting
204 the FITC-dextran width from the total vascular width, then dividing by two. At least three
205 microvessels (< 20 μm width) were measured per each high-powered field.

206 **Fluorescent Activated Cell (FAC) sorting of pulmonary endothelial cells**

207 We excised the whole lung from each animal, and finely minced lung tissue with a
208 scalpel. We then digested the tissue with collagenase type 2 (1000 units/mL) and
209 dispase I (0.125 units/mL) as well as DNase I (0.01 Kunitz units/mL) in HBSS, with
210 agitation for 60 min. We filtered digested tissue through 70 μm filter to remove
211 undigested tissues, and lysed erythrocytes with ACK lysing buffer for 3 min. at 37 $^{\circ}\text{C}$.
212 We washed cells with PBS supplemented with 4% fetal bovine serum, then stained with
213 antibodies against CD31 and CD144 at 1:100 for 40 min. at 4 $^{\circ}\text{C}$ in dark. Live
214 (determined by negative staining for DAPI), double positive population, i.e.
215 CD31 $^{+}$ /CD144 $^{+}$ endothelial cells, were then sorted and lysed immediately after the
216 sorting in lysis buffer supplied in RNeasy Mini Kit. Total RNA was extracted
217 immediately using RNeasy Mini Kit according to manufacturer's protocol. RNA integrity
218 was tested with automated electrophoresis before further analysis.

219 **RNA microarray**

220 Total RNA from pulmonary endothelial cells (CD31 $^{+}$ /CD144 $^{+}$) were used to synthesize
221 cDNA, and cDNA was hybridized to a microarray (Mouse Clariom D, Affymetrix) and

222 scanned with Affymetrix Genechip Scanner 3000. Samples with RNA integrity number
223 greater than 8.7 were used for analysis.

224 **Quantitative Reverse Transcription-Polymerase Chain Reaction (qRT-PCR)**

225 We synthesized cDNA using the iScript cDNA synthesis kit from total RNA isolated from
226 FAC sorted endothelial cells according to manufacturer's protocol. Using Taqman
227 probes, we performed qRT-PCR with the Applied Biosystems 7300 Real-Time PCR
228 System. Cyclophilin (whose expression was unchanged between sham and CLP
229 groups, data not shown) was used as a housekeeping gene, and we analyzed data with
230 the $2^{(-\Delta\Delta Ct)}$ method (17).

231 **Production of recombinant HSulf-1 protein**

232 Recombinant HSulf-1 was expressed as previously described (7). Briefly, HSulf-1
233 coding sequence was inserted in a pcDNA3.1/Myc-His(-) vector, between SNAP and
234 6His tags at the N- and C-terminus, respectively. This vector was used to stably
235 transfect FreeStyle HEK 293-F cells. After harvesting the culture medium, we purified
236 HSulf-1 using two steps of cation-exchange (SP-Sepharose) and size-exclusion
237 chromatography (Superdex-200), as previously described for HSulf-2 (32). After
238 purification, the protein was concentrated over a 30 kDa centrifugal unit, supplemented
239 with 20% glycerol, aliquoted and stored at -20°C.

240 Enzyme activity was assessed as previously described (33), by analyzing the
241 disaccharide composition of untreated and Sulf-treated heparin in trisulfated [UA(2S)-
242 GlcNS(6S)] disaccharide (substrate) and [UA-GlcNS(6S)] disulfated disaccharide

243 (product), using RPIP-HPLC coupled to 2-cyanoacetamide post-column fluorescent
244 derivatization (8).

245 ***In vitro* assays**

246 We cultured primary human pulmonary microvascular endothelial cells using
247 microvascular endothelial growth media. We knocked down Sulf-1 using siRNA
248 targeted to Sulf-1, delivered with Lipofectamine RNAiMax. siRNA was transfected when
249 cells were >80% confluent for 24 h. We harvested cells extracted total RNA using
250 RNeasy Mini kit according to manufacturer's protocol. Cells that were passage 3-6
251 were used for the study.

252 **Statistical analysis**

253 Statistical analysis was performed with GraphPad Prism version 7.0. Single-comparison
254 analyses were performed by t-test; multiple comparisons were performed by one-way
255 ANOVA with Tukey's post-hoc multiple comparisons test. *P*-values less than 0.05 were
256 considered significant. The values are expressed as mean \pm SD.

257 **Results**

258 **Post-septic animals demonstrate impaired inflammatory response to intratracheal**
259 **LPS**

260 To establish a model of post-septic impairment in pulmonary inflammatory responses,
261 we performed cecal ligation and puncture (CLP) or sham surgery. Three days later, we
262 administered 3 µg/g intratracheal (IT) LPS to induce lung inflammation (**Figure 1A**).
263 Compared to sham-operated animals, post-CLP animals showed decreased alveolar
264 leukocyte infiltration (**Figure 1B**) and protein concentration (**Figure 1C**) 2 days after
265 intratracheal LPS. Lung histology from sham-operated animals demonstrated robust
266 intratracheal LPS-induced lung inflammation, including cellular infiltration and alveolar
267 flooding (**Figure 1D**), while such pathology was absent in the lungs of post-CLP animals
268 (**Figure 1E**). Taken together, these findings are consistent with a murine model of
269 CARS.

270 **The post-septic, reconstituted pulmonary endothelial glycocalyx is remodeled**

271 We have previously demonstrated that the pulmonary endothelial glycocalyx, degraded
272 during early sepsis, is reconstituted by 72 h after CLP (45), a time point coincident with
273 our observation of impaired pulmonary inflammatory responses (**Figure 1**). As a simple
274 screen for the presence of HS remodeling, we tested the sensitivity of the post-septic
275 glycocalyx to heparinases with different preferences for sulfated domains of HS.
276 Heparinase-I (which preferentially targets sulfated domains of HS (3)) readily degraded
277 the post-septic and post-sham glycocalyx (**Figure 2A**). In contrast, heparinase-III,
278 which targets undersulfated regions at the periphery of sulfated domains (4), was

279 unable to degrade the post-septic glycoalyx (**Figure 2B**). These findings suggested
280 structural remodeling of the post-septic endothelial glycoalyx.

281 We then directly examined the disaccharide composition of HS comprising the
282 reconstituted pulmonary endothelial glycoalyx (**Figure 2C**). We perfused lungs
283 isolated from mice 72 h after CLP (or sham) with both heparinase I and III for 30 min.
284 We collected the perfusate and measured disaccharide sulfation patterns with HPLC-
285 mass spectrometry multiple reaction monitoring, a high-sensitivity approach capable of
286 detecting ng/ml concentrations of HS (30). HS extracted from the post-septic
287 endothelial glycoalyx demonstrated increased 6-O-sulfation compared to HS isolated
288 from the glycoalyx of sham mice (**Figure 2D**). This post-septic increase in 6-O-
289 sulfation was similarly observed to occur in HS fragments circulating in the blood of
290 mice after CLP (**Figure 2E**). Taken together, these findings suggested that sepsis
291 alters the endothelial machinery responsible for HS disaccharide sulfation, favoring the
292 presence of 6-O-sulfation within the pulmonary vasculature.

293 **Pulmonary endothelial cells in post-septic animals have decreased expression of** 294 **Sulf-1**

295 To determine the presence of transcriptional changes in HS-modifying genes
296 (potentially responsible for the observed increase in 6-O-sulfation detailed in **Figure 2**),
297 we performed FAC sorting to isolate pulmonary endothelial cells (CD31⁺/CD144⁺
298 population) from lungs harvested 48 h after CLP (i.e. immediately prior to remodeling) or
299 sham (**Figure 3A**). Whole RNA transcriptome microarray analyses identified that post-
300 septic pulmonary endothelial cells downregulated expression of sulfatase-1 (Sulf-1)
301 (**Figure 3B**), an enzyme that constitutively removes 6-O-sulfo groups from extracellular

302 HS-chains. Strikingly, there was no difference in other genes that modify 6-O-sulfation
303 of HS, namely sulfatase-2 or HS 6-O-sulfotransferase (microarray data are publically
304 available with GEO accession number: GSE129775). We confirmed these findings in a
305 separate cohort of mice by repeating FAC sorting of pulmonary endothelial cells, then
306 performing qRT-PCR of Sulf-1 (**Figure 3C**).

307 To determine if downregulation of endothelial Sulf-1 similarly occurs after non-septic
308 causes of glycocalyx degradation, we enzymatically degraded endothelial HS from
309 naïve mice by intravenous heparinase III injection (**Figure 3D**). This model leads to
310 rapid endothelial glycocalyx reconstitution within 24 h (45). Twelve hours after
311 heparinase-III (a time point prior to completion of reconstitution), qRT-PCR showed no
312 difference in endothelial Sulf-1 mRNA expression level between heat-inactivated
313 heparinase-III control and heparinase-III treatment groups (**Figure 3E**). These findings
314 suggest that downregulation of endothelial Sulf-1 is a sepsis-specific phenomenon.

315 **Loss of Sulf-1 is necessary for post-septic suppression of pulmonary** 316 **inflammatory responses to intratracheal LPS**

317 Given that loss of endothelial Sulf-1 immediately preceded immunosuppression in post-
318 septic animals, we determined whether loss of Sulf-1 was necessary for CARS. We
319 produced recombinant, enzymatically active Sulf-1 as previously described (7).
320 Resultant Sulf-1 was enzymatically active as evidenced by the 6-O-desulfation of
321 trisulfated [UA(**2S**)-Glc**NS(6S)**] heparin disaccharides (NS2S6S) into [UA(**2S**)-Glc**NS**]
322 disulfated disaccharides (NS2S), monitored by RPIP-HPLC (**Figure 4A**). We induced
323 sepsis in mice by CLP and supplemented surviving animals with exogenous Sulf-1
324 intravenously (3 µg bolus), 2 h prior to intratracheal (IT) LPS challenge (**Figure 4B**).

325 Compared to diluent control group, Sulf-1 treated animals had increased alveolar
326 leukocyte (**Figure 4C**) and protein (**Figure 4D**) concentrations, suggesting reversal of
327 post-septic immunosuppression. Lung histology showed a modest, scattered increase
328 in leukocyte inflammation after IT LPS in post-CLP mice treated with intravenous Sulf-1
329 (**Figure 4E, 4F**). Of note, lungs from Sulf-1 treated animals showed marked
330 perivascular cuffing (**Figure 4F**, black arrows), suggesting restoration of an
331 inflammatory edematous response to LPS. These results suggest that post-septic loss
332 of Sulf-1 is necessary to suppress inflammatory responses to subsequent IT LPS.

333 **Loss of Sulf-1 is not sufficient to induce immunosuppression in non-septic** 334 **animals**

335 We created inducible, endothelial-specific, Sulf-1 and Sulf-2 double knockout mice by
336 breeding Sulf-1^{ff} Sulf-2^{ff} floxed mice with tamoxifen-inducible, endothelial specific
337 VEcadCreERT2 mice to determine whether loss of endothelial Sulf-1 is sufficient to
338 cause impaired pulmonary inflammation. Of note, as Sulf-2 is minimally expressed in
339 the pulmonary endothelium ((24), confirmed by our whole transcriptome experiments,
340 data not shown), endothelial-specific deletion of Sulf-2 is unlikely to impart significant
341 pulmonary impact. We induced recombination with tamoxifen injections for 5
342 consecutive days (1 mg/day, i.p.). After 2 weeks, we first confirmed inducible
343 endothelial-specific recombination with FAC sorting followed by DNA electrophoresis
344 (**Figure 5A**). The cell-specific recombination was confirmed with DNA extracted from
345 FAC sorted endothelial cells (CD31⁺/CD 144⁺) and non-endothelial cells (CD31⁻/CD
346 144⁻) from Sulf-1^{ff} Sulf-2^{ff} VEcadCreERT2⁺ or Sulf-1^{ff} Sulf-2^{ff} VEcadCreERT2⁻ mice,
347 both treated with tamoxifen (**Figure 5B**). These knockout animals had normal blood

348 leukocyte differential and normal coagulation, as measured by CBCs and
349 thromboelastography clot onset time (R-time) respectively (data not shown). There was
350 no evidence of increased pulmonary apoptosis in these mice after tamoxifen treatment
351 (TUNEL staining), and lung histology was unchanged (data not shown). We performed
352 intravital microscopy to determine if the sensitivity of the pulmonary endothelial
353 glycocalyx of tamoxifen-treated, Sulf-1^{ff} Sulf-2^{ff} VEcadCreERT2⁺ mice to enzymatic
354 degradation was similar to that observed in post-septic wild-type mice (**Figure 2B**). The
355 pulmonary endothelial glycocalyx of these Sulf-1 and -2 double knockout mice
356 demonstrated resistance to heparinase-III (**Figure 5C**), but not against heparinase I
357 (data not shown), confirming similar glycocalyx remodeling as observed in post-septic
358 mice (**Figure 2A, 2B**).

359 We challenged tamoxifen-treated Sulf-1^{ff} Sulf-2^{ff} VEcadCreERT2⁺ mice with IT LPS to
360 determine whether endothelial-specific Sulf-1/Sulf-2 knockout is sufficient to impair
361 pulmonary inflammatory responses in non-septic mice, (**Figure 5A**). There was no
362 difference between control group animals and double knockout animals in leukocytes
363 numbers (**Figure 5D**) and protein concentration (**Figure 5E**) in BAL fluid. Similarly,
364 there was no obvious difference observed in lung histology between the control group
365 (**Figures 5F**) and Sulf-1/2 knockout group (**Figure 5G**). Taken together, the data
366 indicated that loss of Sulf-1 is not sufficient to cause impaired pulmonary inflammation
367 in non-septic animals.

368 **Sulf-1 silencing in human primary pulmonary microvascular endothelial cells**
369 **results in decreased mRNA expression of ICAM-1**

370 6-O-sulfation may impact numerous biological pathways, spanning growth factor,
371 chemokine, and damage-associated molecular pattern signaling (5). We used siRNA
372 approaches to knock down Sulf-1 in primary human microvascular endothelial cells to
373 determine if the consequences of Sulf-1 loss on these signaling pathways converge to
374 impart a general anti-inflammatory phenotype to endothelial cells. We cultured primary
375 human lung microvascular endothelial cells in a 6-well plate, and transfected siRNA
376 using lipofectamine. We performed three biological replicates, each of which
377 represented cells collected from a separate human donor. Our transfection resulted in
378 greater than 83% knock down efficiency (**Figure 6A**). We examined whether a major
379 adhesion molecule for neutrophil adhesion, ICAM-1, was affected by this knockdown.
380 Loss of Sulf-1 resulted in downregulation of ICAM-1 expression in endothelial cells
381 (**Figure 6B**). These findings suggest that loss of Sulf-1 may drive pathways that
382 suppress endothelial activation. As these unstimulated endothelial cells expressed little
383 ICAM-1 protein at baseline (data not shown), we are unable to demonstrate a direct
384 effect of loss of Sulf-1 on endothelial-leukocyte adhesion.

385

386 **Discussion**

387 In this study, we demonstrated that post-CLP mice have impaired alveolar
388 inflammation in response to intratracheal LPS. This post-septic “immunoparalysis”
389 coincides with reconstitution of a remodeled pulmonary endothelial glycocalyx, as
390 demonstrated by differential sensitivity to enzymatic degradation during intravital
391 microscopy and enrichment in 6-O-sulfated HS monitored by mass spectrometry.
392 These changes coincide with selective pulmonary endothelial downregulation of Sulf-1,

393 an enzyme dedicated to the constitutive removal of 6-O-sulfo groups. We observed that
394 loss of Sulf-1 is necessary for impaired inflammation in post-septic animals, but it alone
395 was not sufficient to cause impaired inflammation in non-septic animals. Our data
396 therefore collectively indicate an endothelial role in CARS, a syndrome to date largely
397 relegated to post-septic leukocyte dysfunction.

398 Our findings indicate that sepsis suppresses endothelial Sulf-1, impairing
399 subsequent inflammatory responses after the resolution of septic endothelial injury.
400 Teleologically, this response may be designed to limit the degree of lung injury, shifting
401 endothelial signaling towards tissue repair. For example, an increase in 6-O-sulfation
402 promotes cell response to HS-binding growth factors, FGF2 and VEGF, which may
403 promote endothelial repair processes (6). However, this response may backfire if the
404 host is exposed to a secondary infection, by attenuating host-protective antimicrobial
405 responses. Post-septic patients are susceptible to secondary infection, with hospital-
406 acquired pneumonia the most common complication (15, 39). Septic patients who later
407 acquired secondary infections experience more severe illness, longer length-of-stay,
408 and higher 1-year mortality (39, 40). Therefore, in the presence of hospital-acquired
409 infection, loss of endothelial Sulf-1 may be detrimental. Additionally, we found that post-
410 septic animals had increased absolute neutrophil count in blood at the time of
411 intratracheal LPS (data not shown), indicating that decreased neutrophil infiltration
412 found in BAL fluid is not due to post-septic depletion of circulating neutrophils.
413 Interestingly, when the whole transcriptome profiles from circulating leukocytes were
414 compared between patients who acquired secondary infection and those who did not,
415 there was no difference in pro- or anti-inflammatory genes (39). However, there was

416 significant increase in plasma proteins, including circulating cytokines, such as IL-8 and
417 IL-10, and markers of vascular dysfunction and activation, such as E-selectin,
418 angiopoietins, ICAM-1, and proteins that promote coagulation in patients who
419 developed secondary infections, compared to the patients who did not (40). Taken
420 together, these findings suggest that CARS is most likely more complex than leukocyte
421 dysfunction, and warrant further investigations to determine contributions by other cells
422 and organs such as vascular endothelial cells.

423 Although we have shown one potential effect of loss of Sulf-1, i.e. endothelial
424 ICAM-1 downregulation, the mechanisms by which loss of Sulf-1 results in impaired
425 inflammation remain uncertain. Sulf-1 and Sulf-2 are unique in that they are the only
426 extracellular sulfatases modifying HS at the post-synthetic level, suggesting a critical
427 importance of 6-O-sulfation for the function of glycocalyx HS. Indeed, 6-O-sulfation may
428 influence numerous biological processes of consequence, including growth factor,
429 chemokine, and damage-associated molecular pattern signaling (5). One possible
430 mechanism is that a shift in 6-O-sulfation affects the affinity of endothelial HS to
431 cytokines that modulate neutrophil infiltration. Sulf-2 is shown to selectively mobilize not
432 only specific growth factors but also cytokines (such as SDF-1 and SLC) that impact
433 neutrophil migration (36, 38). Changes in endothelial HS 6-O-sulfation shape the
434 microenvironment and inflammatory response in multiple ways, given their multiple
435 biological roles. Changes in HS sulfation may result in altered systemic immunity, and
436 enhanced bacterial adhesion to endothelial cells (43). Although the roles of endothelial
437 selectins to neutrophil extravasation in pulmonary circulation are complex (13, 20), it
438 has been reported that changes in sulfation in endothelial HS, particularly 6-O-sulfation,

439 weakens neutrophil binding to L-selectin and P-selectin (41, 42). Accordingly, the
440 immunosuppressive effects of loss of Sulf-1 may arise from numerous potential
441 processes, potentially converging upon pathways such as adhesion molecule
442 expression (**Figure 6**). Future studies will screen for 6-O-sulfated HS binding proteins,
443 providing greater insight into the downstream mechanisms responsible for our observed
444 effects of Sulf-1 on post-septic pulmonary inflammation.

445 An additional consideration is that changes in endothelial Sulf-1/2 expression
446 may impact the dynamics of glycocalyx degradation. Indeed, our endothelial microarray
447 experiments (GEO accession number: GSE129775) demonstrated that post-septic (48
448 h) loss of Sulf-1 coincided with increased expression of matrix metalloproteinases 8, 9,
449 25, and disintegrin and metalloproteinase domain-containing proteins 8, 15, 23. No
450 changes were seen in endothelial expression of heparanase or matrix metalloproteinase
451 15 in these post-septic mice. Future studies will be required to investigate the presence
452 of sulfatase-sheddase cross-talk and its relevance to lung injury and repair.

453 Sulf-1 and Sulf-2 preferentially targets trisulfated, NS2S6S disaccharides of HS,
454 and to a lesser extent, NS6S (22). Loss of Sulf-1, therefore, would be expected to
455 result in an increase of trisulfated, NS2S6S disaccharides (substrate), with a decrease
456 in NS2S (product). However, we rather observed an increase of HS overall 6-O-
457 sulfation (**Figure 2D**). This discrepancy may reflect the additional ability of Sulf-1 and
458 Sulf-2 to directly regulate HS biosynthesis enzymes (14). Therefore, it is possible that
459 our biological observations following Sulf-1 downregulation may be caused directly by
460 the loss of Sulf-1 activity, and/or indirectly, through a regulation of HS biosynthesis. Of
461 note, our recombinant Sulf-1 is of human origin. Based on the strong sequence

462 homology of HSulf-1 and MSulf-1, we do not expect any significant differences in
463 enzymatic activity (22), but we cannot exclude the possibility that enzymatic activity is
464 slightly different *in vivo*.

465 In conclusion, our study showed that post-septic pulmonary endothelial
466 glycocalyx HS undergoes structural remodeling, coincident with loss of endothelial Sulf-
467 1. Although loss of Sulf-1 in endothelial cells is not sufficient to cause impaired
468 inflammation in non-septic mice, it contributes to post-septic CARS, offering a potential
469 new target for treating post-septic patients at risk for nosocomial pneumonia.

470 **Acknowledgement**

471 We would like to thank technical help from the Genomics and Microarray Core and from
472 the CU Cancer Center Flow Cytometry Shared Resource at University of Colorado
473 Denver. We would also like to thank Dr. Ralf Adams at Max Planck Institute, Germany,
474 for generously providing VEcadhein-CRE-ERT2 mice.

475

476 **Funding**

477 This work was supported by Department of Defense (CDMRP) grant PR150655 (to Dr.
478 Schmidt), NIH grant R01 HL125371 (to Drs. Schmidt and Linhardt). In addition, work
479 performed by Dr. Vivès was supported by the CNRS and the GDR GAG (GDR 3739),
480 the “Investissements d’avenir” program Glyco@Alps (ANR-15-IDEX-02), and by grants
481 from the Agence Nationale de la Recherche (ANR-17-CE11-0040) and Université
482 Grenoble-Alpes (UGA AGIR program). Hematologic analyses were supported by
483 Maternal Child Health Bureau Grant H30MC24049 (to Dr. Davizon-Castillo).

484

485 **Disclosure**

486 None.

487 **Figure Legends**

488 **Figure 1: Post-CLP mice demonstrate suppressed inflammatory response to**

489 **intratracheal lipopolysaccharide.** (A) We performed cecal ligation and puncture

490 (CLP) or sham surgery on day 0. Three days after surgery, we challenged animals with

491 intratracheal (IT) lipopolysaccharides (LPS) (3 $\mu\text{g/g}$ body weight). Animals were

492 harvested 2 days after IT LPS. (B) Post-CLP animals had decreased number of

493 leukocytes per mL in bronchoalveolar lavage (BAL) fluid 2 days after intratracheal LPS.

494 (C) Post-CLP animals demonstrated less alveolar injury 2 days after intratracheal LPS,

495 based on protein concentrations in BAL fluid. (D) Lung histological section from a sham

496 animal (stained with H&E) showed evidence of lung inflammation 2 days after

497 intratracheal LPS. (E) Lung histological section from a CLP animal (stained with H&E) 2

498 days after intratracheal LPS showed minimal evidence of lung inflammation. Scale bars

499 on lower magnification images = 500 μm and those on higher magnification images

500 =100 μm . $n= 5$ each group, Student's t-test, $*P < 0.05$.

501 **Figure 2: The post-septic, reconstituted endothelial glycocalyx is remodeled.** (A)

502 At the 72 h time point characterized by pulmonary endothelial HS reconstitution, we

503 injected 1 unit of heparinase I (Hep I) into the jugular vein, which degraded both sham

504 and post-CLP pulmonary endothelial glycocalyx heparan sulfate. (B) In contrast, 1 unit

505 of heparinase III (Hep III) into the jugular vein did not degrade post-septic pulmonary

506 endothelial heparan sulfate. (C) Major sulfation positions on heparan sulfate constituent

507 disaccharides. (D) Post-septic, reconstituted pulmonary endothelial heparan sulfate

508 had a significantly increase ($P < 0.05$) in disaccharides with 6-O-sulfation (percentage of

509 total sulfated disaccharides) as compared to heparan sulfate from sham animals. (E)

510 The percentage of 6-O-sulfated disaccharides increased over time in the plasma of
511 post-CLP mice. ESL: endothelial surface layer. n= 3-5 per group, Student's t-test, * $P <$
512 0.05.

513 **Figure 3: Post-septic pulmonary endothelial cells downregulate Sulf-1 mRNA.** (A)
514 We collected pulmonary endothelial cells and extracted total RNA at day 2, a time point
515 immediately prior to glycocalyx reconstitution at day 3. (B) Pulmonary endothelial cells
516 in mice 48 h after CLP had decreased Sulf-1 expression detected with RNA microarray.
517 (C) We validated the downregulation of Sulf-1 in pulmonary endothelial cells by qRT-
518 PCR using separate biological replicates. (D) We collected pulmonary endothelial cells
519 and extracted total RNA at 12 h after heparinase III injection, a time point immediately
520 prior to glycocalyx reconstitution after enzymatic, non-septic degradation. (E) mRNA
521 expression level of Sulf-1 in pulmonary endothelial cells were similar 12 h after
522 enzymatic degradation by heparinase III (Hep III) or heat-inactivated (HI) Hep III. n= 3-4
523 each group, Student's t-test, * $P <$ 0.05.

524 **Figure 4: Loss of Sulf-1 contributes to post-septic CARS.** (A) Recombinant Sulf-1
525 was enzymatically active and efficiently removed 6-O sulfates from heparin, as shown
526 by the decrease in trisulfated [UA(2S)-GlcNS(6S)] disaccharide content (NS2S6S) and
527 concomitant increase of [UA-GlcNS(6S)] disulfated disaccharide (NS2S) in Sulf-1
528 treated heparin (white bars) compared to untreated control (black bars). (B) We
529 performed CLP on mice on day 0. On day 3, surviving post-septic mice were treated
530 with intravenous (IV) Sulf-1 (3 μ g bolus) or diluent, then challenged with intratracheal
531 (IT) LPS (3 μ g/g body weight). Animals were harvested 2 days after IT LPS. (C) Sulf-1
532 treated animals had increased leukocytes in BAL fluid 2 days after IT LPS, as compared

533 to diluent treated animals 2 days after IT LPS. (D) Sulf-1 treated animals also showed
534 increased lung injury based on protein concentration in BAL fluid. (E) Lung histological
535 section from a post-septic, diluent treated animal (stained with H&E) showed very little
536 evidence of lung inflammation. (F) Lung histological section from a post-septic Sulf-1
537 treated animal (stained with H&E) showed increased tissue consolidation 2 days after IT
538 LPS. In addition, Sulf-1 treated animals had marked perivascular cuffs (black arrows).
539 Scale bars on lower magnification images = 500 μm and those on higher magnification
540 images = 100 μm . $n = 4-5$ each group, Student's t-test, $*P < 0.05$.

541 **Figure 5: Loss of Sulf-1 is not sufficient to cause impaired inflammation in non-**
542 **septic animals.** (A) Sulf-1^{ff} Sulf-2^{ff} VEcadCreERT2^{+ or -} animals received tamoxifen or
543 vehicle control injections intraperitoneally for 5 consecutive days (1 mg/day).
544 Recombination of genes and pulmonary endothelial glycocalyx characteristics were
545 evaluated 2 weeks after the last injection of tamoxifen (or vehicle). Knockout or control
546 mice were alternatively challenged with IT LPS (3 $\mu\text{g}/\text{g}$ body weight) at the same time
547 point. (B) We confirmed cell-specific, inducible recombination of Sulf-1 and Sulf-2 with
548 DNA gels. Lane 1: DNA from pulmonary non-endothelial cells (CD31-/CD144-), Lane 2:
549 DNA from pulmonary endothelial cells (CD31+/CD144+). (C) Pulmonary endothelial
550 glycocalyx of Sulf-1/2 knockout animals was resistant to heparinase III (Hep III)
551 degradation, similar to the post-septic endothelial glycocalyx resistance to heparinase III
552 observed in wild-type mice (**Figure 2B**). Control animals used were Sulf-1^{ff} Sulf-2^{ff}
553 VEcadCreERT2⁻ (floxed gene alone without Cre recombinase), treated with tamoxifen.
554 (D) Number of leukocytes in BAL fluid in Sulf-1/2 knockout animals did not differ from
555 control groups 2 days after IT LPS. (E) Protein concentration of BAL fluid was similarly

556 not different among the experimental groups. (F) Lung histological section from a
557 control animal (Sulf-1^{ff} Sulf-2^{ff} VEcadCreERT2⁻, treated with tamoxifen) had clear
558 consolidation. (G) Lung histological section from a Sulf-1/2 knockout animal similarly
559 had evidence of lung inflammation. Scale bars on lower magnification images = 500 μ m
560 and those on higher magnification images = 100 μ m. n = 3-6 each group, One-way
561 ANOVA with post hoc Turkey test, * P < 0.05.

562 **Figure 6: Knocking down Sulf-1 in pulmonary microvascular endothelial cells**
563 **decreases ICAM-1 expression.** (A) We transfected cultured endothelial cells with
564 siRNA targeted to Sulf-1 using Lipofectamine RNAiMAX for 24 hours, which resulted in
565 greater than 83% knockdown of Sulf-1. (B) Knock down of Sulf-1 resulted in
566 downregulation of ICAM-1 expression in endothelial cells. Control cells were treated
567 with lipofectamine without siRNA. n = 3, each data point represents average of 2-3
568 wells per treatment. Student's t-test, * P < 0.05.

569 **References:**

- 570 1. **Bone RC, Grodzin CJ, and Balk RA.** Sepsis: a new hypothesis for
571 pathogenesis of the disease process. *Chest* 112: 235-243, 1997.
- 572 2. **Boomer JS, To K, Chang KC, Takasu O, Osborne DF, Walton AH, Bricker TL,**
573 **Jarman SD, 2nd, Kreisel D, Krupnick AS, Srivastava A, Swanson PE, Green JM,**
574 **and Hotchkiss RS.** Immunosuppression in patients who die of sepsis and multiple
575 organ failure. *JAMA* 306: 2594-2605, 2011.
- 576 3. **Desai UR, Wang HM, and Linhardt RJ.** Specificity studies on the heparin lyases
577 from *Flavobacterium heparinum*. *Biochemistry* 32: 8140-8145, 1993.
- 578 4. **Desai UR, Wang HM, and Linhardt RJ.** Substrate specificity of the heparin
579 lyases from *Flavobacterium heparinum*. *Arch Biochem Biophys* 306: 461-468, 1993.
- 580 5. **El Masri R, Seffouh A, Lortat-Jacob H, and Vives RR.** The "in and out" of
581 glucosamine 6-O-sulfation: the 6th sense of heparan sulfate. *Glycoconj J* 34: 285-298,
582 2017.
- 583 6. **Ferreras C, Rushton G, Cole CL, Babur M, Telfer BA, van Kuppevelt TH,**
584 **Gardiner JM, Williams KJ, Jayson GC, and Avizienyte E.** Endothelial heparan sulfate
585 6-O-sulfation levels regulate angiogenic responses of endothelial cells to fibroblast
586 growth factor 2 and vascular endothelial growth factor. *J Biol Chem* 287: 36132-36146,
587 2012.
- 588 7. **Heidari-Hamedani G, Vives RR, Seffouh A, Afratis NA, Oosterhof A, van**
589 **Kuppevelt TH, Karamanos NK, Metintas M, Hjerpe A, Dobra K, and Szatmari T.**
590 Syndecan-1 alters heparan sulfate composition and signaling pathways in malignant
591 mesothelioma. *Cell Signal* 27: 2054-2067, 2015.
- 592 8. **Henriet E, Jager S, Tran C, Bastien P, Michelet JF, Minondo AM, Formanek**
593 **F, Dalko-Csiba M, Lortat-Jacob H, Breton L, and Vives RR.** A jasmonic acid
594 derivative improves skin healing and induces changes in proteoglycan expression and
595 glycosaminoglycan structure. *Biochim Biophys Acta Gen Subj* 1861: 2250-2260, 2017.
- 596 9. **Hotchkiss RS, and Opal S.** Immunotherapy for sepsis--a new approach against
597 an ancient foe. *The New England journal of medicine* 363: 87-89, 2010.
- 598 10. **Hynninen M, Pettila V, Takkunen O, Orko R, Jansson SE, Kuusela P,**
599 **Renkonen R, and Valtonen M.** Predictive value of monocyte histocompatibility
600 leukocyte antigen-DR expression and plasma interleukin-4 and -10 levels in critically ill
601 patients with sepsis. *Shock* 20: 1-4, 2003.
- 602 11. **Jastrebova N, Vanwildemeersch M, Lindahl U, and Spillmann D.** Heparan
603 sulfate domain organization and sulfation modulate FGF-induced cell signaling. *J Biol*
604 *Chem* 285: 26842-26851, 2010.
- 605 12. **Kempker JA, and Martin GS.** The Changing Epidemiology and Definitions of
606 Sepsis. *Clin Chest Med* 37: 165-179, 2016.
- 607 13. **Kolaczowska E, and Kubes P.** Neutrophil recruitment and function in health
608 and inflammation. *Nat Rev Immunol* 13: 159-175, 2013.
- 609 14. **Lamanna WC, Frese MA, Balleininger M, and Dierks T.** Sulf loss influences N-,
610 2-O-, and 6-O-sulfation of multiple heparan sulfate proteoglycans and modulates
611 fibroblast growth factor signaling. *J Biol Chem* 283: 27724-27735, 2008.

- 612 15. **Landelle C, Lepape A, Voirin N, Tognet E, Venet F, Bohe J, Vanhems P, and**
613 **Monneret G.** Low monocyte human leukocyte antigen-DR is independently associated
614 with nosocomial infections after septic shock. *Intensive Care Med* 36: 1859-1866, 2010.
- 615 16. **Lekkou A, Karakantza M, Mouzaki A, Kalfarentzos F, and Gogos CA.**
616 Cytokine production and monocyte HLA-DR expression as predictors of outcome for
617 patients with community-acquired severe infections. *Clin Diagn Lab Immunol* 11: 161-
618 167, 2004.
- 619 17. **Livak KJ, and Schmittgen TD.** Analysis of relative gene expression data using
620 real-time quantitative PCR and the 2(-Delta Delta C(T)) Method. *Methods* 25: 402-408,
621 2001.
- 622 18. **Marshall JC.** Why have clinical trials in sepsis failed? *Trends Mol Med* 20: 195-
623 203, 2014.
- 624 19. **Meisel C, Schefold JC, Pschowski R, Baumann T, Hetzger K, Gregor J,**
625 **Weber-Carstens S, Hasper D, Keh D, Zuckermann H, Reinke P, and Volk HD.**
626 Granulocyte-macrophage colony-stimulating factor to reverse sepsis-associated
627 immunosuppression: a double-blind, randomized, placebo-controlled multicenter trial.
628 *Am J Respir Crit Care Med* 180: 640-648, 2009.
- 629 20. **Mizgerd JP, Meek BB, Kutkoski GJ, Bullard DC, Beaudet AL, and**
630 **Doerschuk CM.** Selectins and neutrophil traffic: margination and *Streptococcus*
631 *pneumoniae*-induced emigration in murine lungs. *J Exp Med* 184: 639-645, 1996.
- 632 21. **Monneret G, Finck ME, Venet F, Debard AL, Bohe J, Bienvenu J, and**
633 **Lepape A.** The anti-inflammatory response dominates after septic shock: association of
634 low monocyte HLA-DR expression and high interleukin-10 concentration. *Immunol Lett*
635 95: 193-198, 2004.
- 636 22. **Morimoto-Tomita M, Uchimura K, Werb Z, Hemmerich S, and Rosen SD.**
637 Cloning and characterization of two extracellular heparin-degrading endosulfatases in
638 mice and humans. *J Biol Chem* 277: 49175-49185, 2002.
- 639 23. **Munoz C, Carlet J, Fitting C, Misset B, Bleriot JP, and Cavaillon JM.**
640 Dysregulation of in vitro cytokine production by monocytes during sepsis. *J Clin Invest*
641 88: 1747-1754, 1991.
- 642 24. **Nagamine S, Tamba M, Ishimine H, Araki K, Shiomi K, Okada T, Ohto T,**
643 **Kunita S, Takahashi S, Wismans RG, van Kuppevelt TH, Masu M, and Keino-Masu**
644 **K.** Organ-specific sulfation patterns of heparan sulfate generated by extracellular
645 sulfatases Sulf1 and Sulf2 in mice. *J Biol Chem* 287: 9579-9590, 2012.
- 646 25. **Nakos G, Malamou-Mitsi VD, Lachana A, Karassavoglou A, Kitsioulis E,**
647 **Agnandi N, and Lekka ME.** Immunoparalysis in patients with severe trauma and the
648 effect of inhaled interferon-gamma. *Crit Care Med* 30: 1488-1494, 2002.
- 649 26. **Otto GP, Sossdorf M, Claus RA, Rodel J, Menge K, Reinhart K, Bauer M,**
650 **and Riedemann NC.** The late phase of sepsis is characterized by an increased
651 microbiological burden and death rate. *Crit Care* 15: R183, 2011.
- 652 27. **Reine TM, Kusche-Gullberg M, Feta A, Jenssen T, and Kolset SO.** Heparan
653 sulfate expression is affected by inflammatory stimuli in primary human endothelial cells.
654 *Glycoconj J* 29: 67-76, 2012.
- 655 28. **Sarrazin S, Lamanna WC, and Esko JD.** Heparan sulfate proteoglycans. *Cold*
656 *Spring Harb Perspect Biol* 3: 2011.

- 657 29. **Schmidt EP, Damarla M, Rentsendorj O, Servinsky LE, Zhu B, Moldobaeva**
658 **A, Gonzalez A, Hassoun PM, and Pearse DB.** Soluble guanylyl cyclase contributes to
659 ventilator-induced lung injury in mice. *Am J Physiol Lung Cell Mol Physiol* 295: L1056-
660 1065, 2008.
- 661 30. **Schmidt EP, Overdier KH, Sun X, Lin L, Liu X, Yang Y, Ammons LA, Hiller**
662 **TD, Suflita MA, Yu Y, Chen Y, Zhang F, Cothren Burlew C, Edelstein CL, Douglas**
663 **IS, and Linhardt RJ.** Urinary Glycosaminoglycans Predict Outcomes in Septic Shock
664 and Acute Respiratory Distress Syndrome. *Am J Respir Crit Care Med* 194: 439-449,
665 2016.
- 666 31. **Schmidt EP, Yang Y, Janssen WJ, Gandjeva A, Perez MJ, Barthel L,**
667 **Zemans RL, Bowman JC, Koyanagi DE, Yunt ZX, Smith LP, Cheng SS, Overdier**
668 **KH, Thompson KR, Geraci MW, Douglas IS, Pearse DB, and Tuder RM.** The
669 pulmonary endothelial glycocalyx regulates neutrophil adhesion and lung injury during
670 experimental sepsis. *Nat Med* 18: 1217-1223, 2012.
- 671 32. **Seffouh A, El Masri R, Makshakova O, Gout E, Hassoun ZEO, Andrieu JP,**
672 **Lortat-Jacob H, and Vives RR.** Expression and purification of recombinant
673 extracellular sulfatase HSulf-2 allows deciphering of enzyme sub-domain coordinated
674 role for the binding and 6-O-desulfation of heparan sulfate. *Cell Mol Life Sci* 2019.
- 675 33. **Seffouh I, Przybylski C, Seffouh A, El Masri R, Vives RR, Gonnet F, and**
676 **Daniel R.** Mass spectrometry analysis of the human endosulfatase HSulf-2. *Biochem*
677 *Biophys Rep* 18: 100617, 2019.
- 678 34. **Singer M, Deutschman CS, Seymour CW, Shankar-Hari M, Annane D, Bauer**
679 **M, Bellomo R, Bernard GR, Chiche JD, Coopersmith CM, Hotchkiss RS, Levy MM,**
680 **Marshall JC, Martin GS, Opal SM, Rubenfeld GD, van der Poll T, Vincent JL, and**
681 **Angus DC.** The Third International Consensus Definitions for Sepsis and Septic Shock
682 (Sepsis-3). *JAMA* 315: 801-810, 2016.
- 683 35. **Stephan F, Yang K, Tankovic J, Soussy CJ, Dhonneur G, Duvaldestin P,**
684 **Brochard L, Brun-Buisson C, Harf A, and Delclaux C.** Impairment of
685 polymorphonuclear neutrophil functions precedes nosocomial infections in critically ill
686 patients. *Crit Care Med* 30: 315-322, 2002.
- 687 36. **Suratt BT, Petty JM, Young SK, Malcolm KC, Lieber JG, Nick JA, Gonzalo**
688 **JA, Henson PM, and Worthen GS.** Role of the CXCR4/SDF-1 chemokine axis in
689 circulating neutrophil homeostasis. *Blood* 104: 565-571, 2004.
- 690 37. **Tran TH, Shi X, Zaia J, and Ai X.** Heparan sulfate 6-O-endosulfatases (Sulfs)
691 coordinate the Wnt signaling pathways to regulate myoblast fusion during skeletal
692 muscle regeneration. *J Biol Chem* 287: 32651-32664, 2012.
- 693 38. **Uchimura K, Morimoto-Tomita M, Bistrup A, Li J, Lyon M, Gallagher J, Werb**
694 **Z, and Rosen SD.** HSulf-2, an extracellular endoglucosamine-6-sulfatase, selectively
695 mobilizes heparin-bound growth factors and chemokines: effects on VEGF, FGF-1, and
696 SDF-1. *BMC Biochem* 7: 2, 2006.
- 697 39. **van Vught LA, Klein Klouwenberg PM, Spitoni C, Scicluna BP, Wiewel MA,**
698 **Horn J, Schultz MJ, Nurnberg P, Bonten MJ, Cremer OL, van der Poll T, and**
699 **Consortium M.** Incidence, Risk Factors, and Attributable Mortality of Secondary
700 Infections in the Intensive Care Unit After Admission for Sepsis. *JAMA* 315: 1469-1479,
701 2016.

- 702 40. **van Vught LA, Wiewel MA, Hoogendijk AJ, Frencken JF, Scicluna BP, Klein**
703 **Klouwenberg PMC, Zwinderman AH, Lutter R, Horn J, Schultz MJ, Bonten MMJ,**
704 **Cremer OL, and van der Poll T.** The Host Response in Patients with Sepsis
705 Developing Intensive Care Unit-acquired Secondary Infections. *Am J Respir Crit Care*
706 *Med* 196: 458-470, 2017.
- 707 41. **Wang L, Brown JR, Varki A, and Esko JD.** Heparin's anti-inflammatory effects
708 require glucosamine 6-O-sulfation and are mediated by blockade of L- and P-selectins.
709 *J Clin Invest* 110: 127-136, 2002.
- 710 42. **Wang L, Fuster M, Sriramarao P, and Esko JD.** Endothelial heparan sulfate
711 deficiency impairs L-selectin- and chemokine-mediated neutrophil trafficking during
712 inflammatory responses. *Nat Immunol* 6: 902-910, 2005.
- 713 43. **Xu D, Olson J, Cole JN, van Wijk XM, Brinkmann V, Zychlinsky A, Nizet V,**
714 **Esko JD, and Chang YC.** Heparan Sulfate Modulates Neutrophil and Endothelial
715 Function in Antibacterial Innate Immunity. *Infect Immun* 83: 3648-3656, 2015.
- 716 44. **Xu PB, Lou JS, Ren Y, Miao CH, and Deng XM.** Gene expression profiling
717 reveals the defining features of monocytes from septic patients with compensatory anti-
718 inflammatory response syndrome. *J Infect* 65: 380-391, 2012.
- 719 45. **Yang Y, Haeger SM, Suflita MA, Zhang F, Dailey KL, Colbert JF, Ford JA,**
720 **Picon MA, Stearman RS, Lin L, Liu X, Han X, Linhardt RJ, and Schmidt EP.**
721 Fibroblast Growth Factor Signaling Mediates Pulmonary Endothelial Glycocalyx
722 Reconstitution. *Am J Respir Cell Mol Biol* 56: 727-737, 2017.

723

Figure 1 CARS model

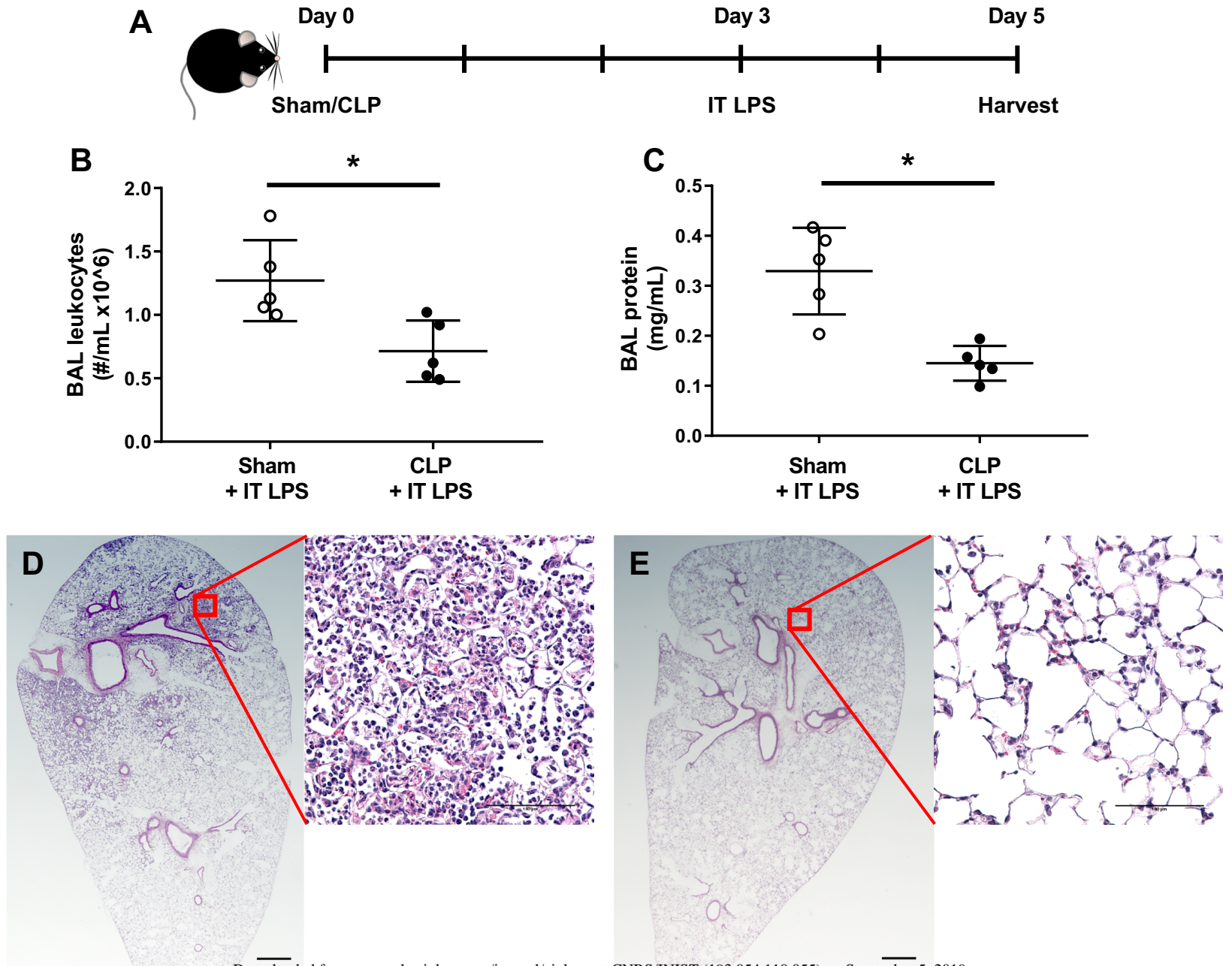


Figure 2 Post-septic, reconstituted glycolyx acquires increased 6-O sulfation and newly found resistance against heparinase III digestion, but not against heparinase I

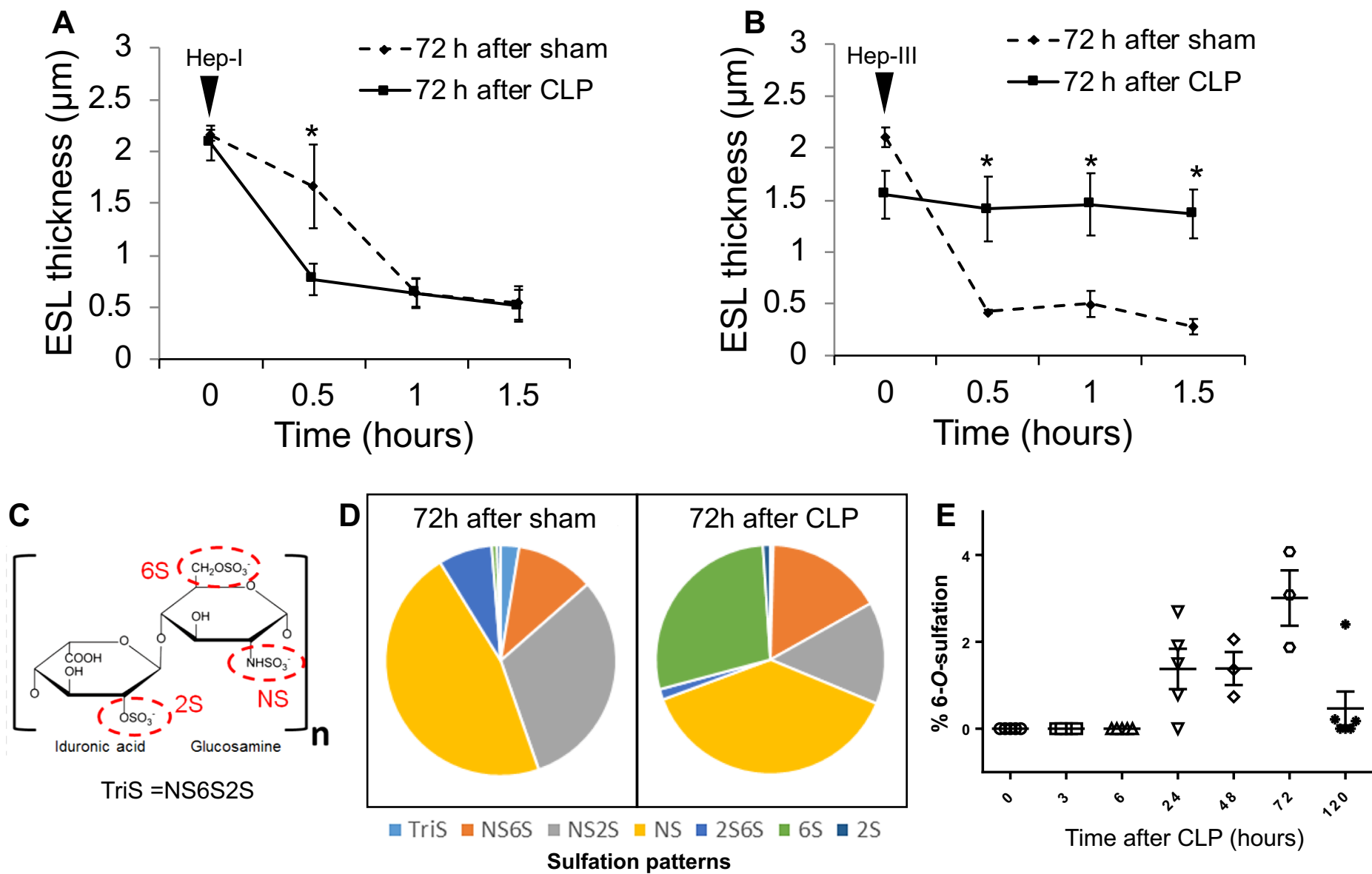


Figure 3 Post-septic pulmonary endothelial cells downregulate Sulf-1

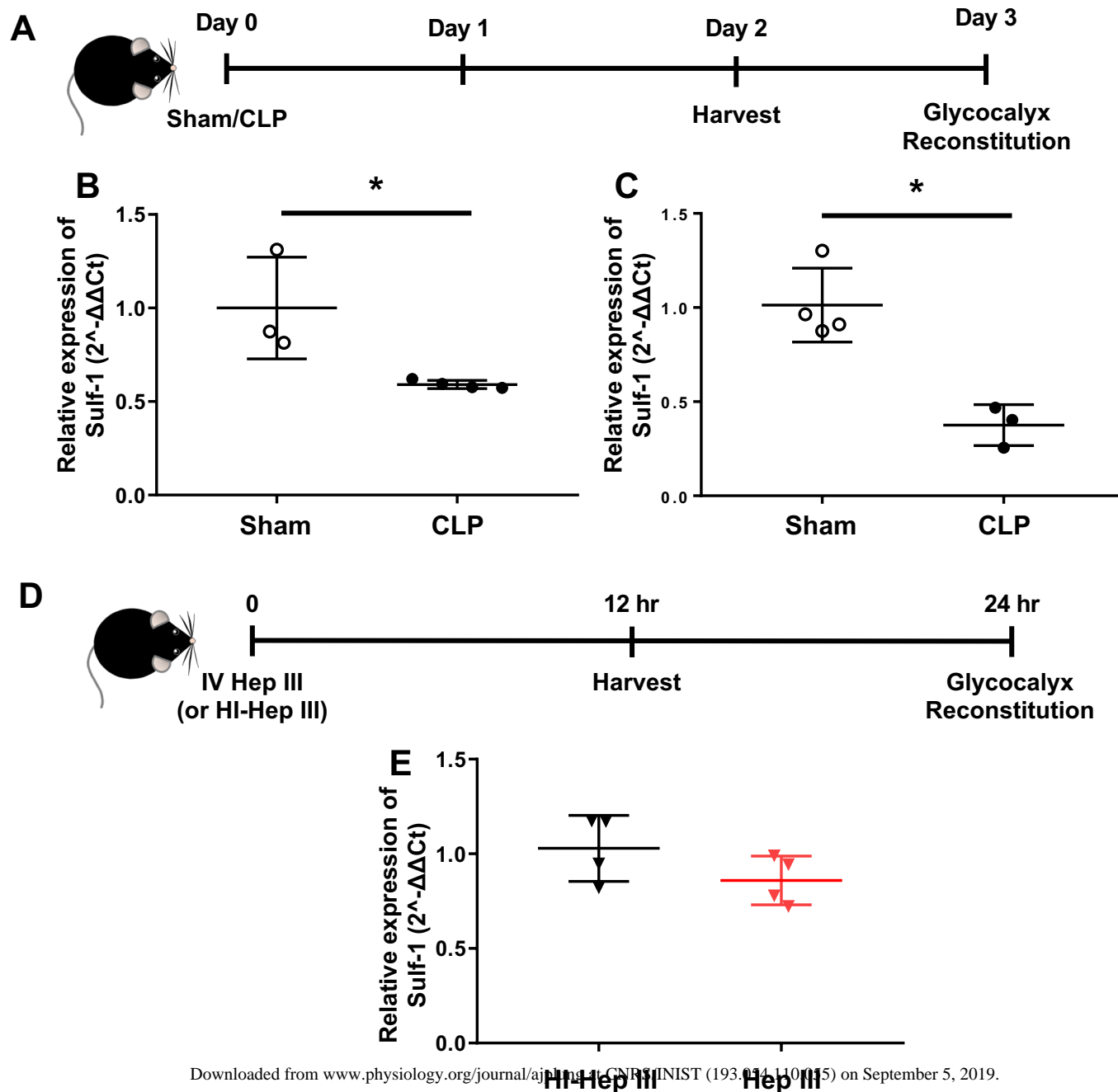


Figure 4 Sulf-1 is necessary for CARS

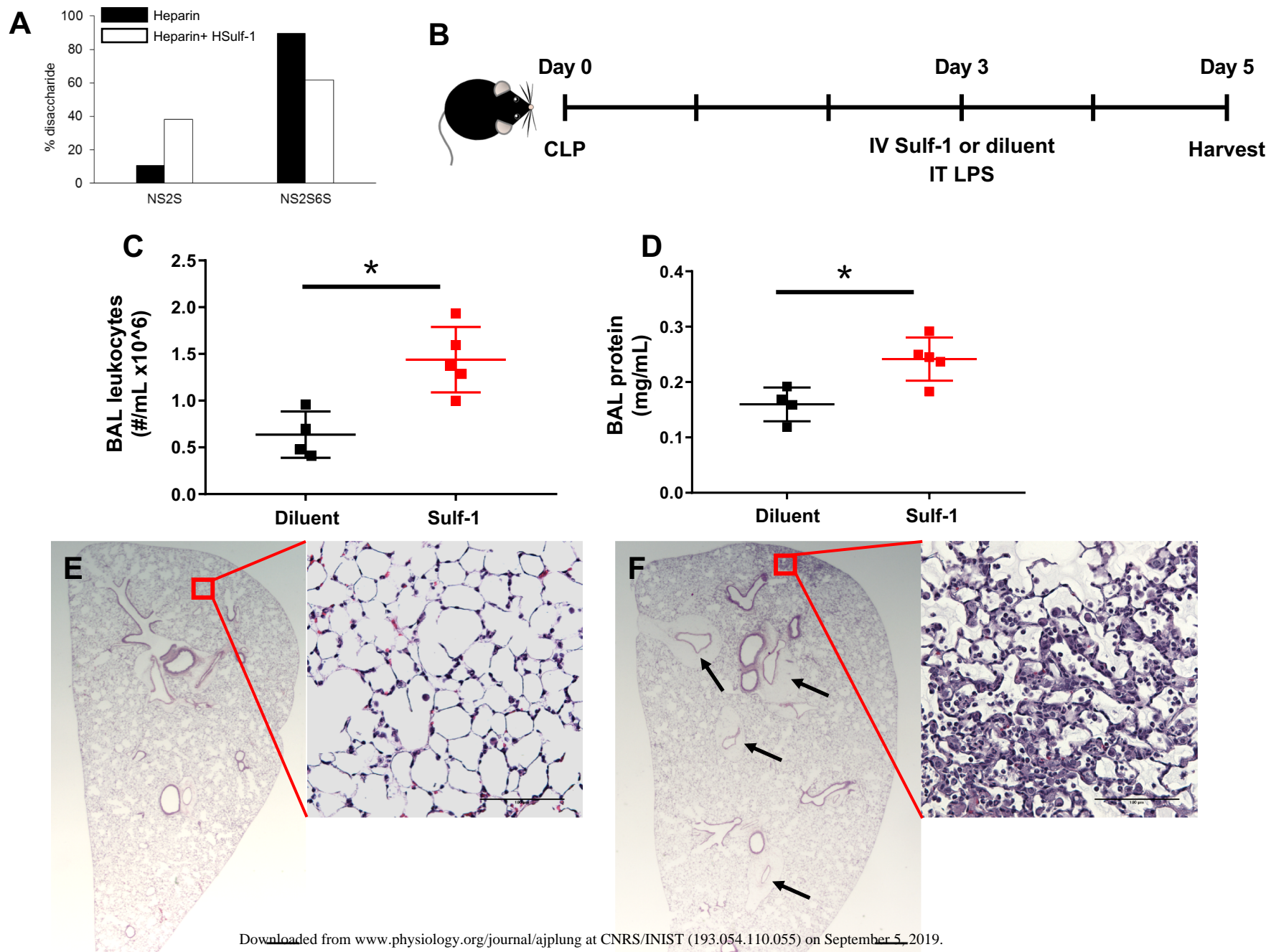
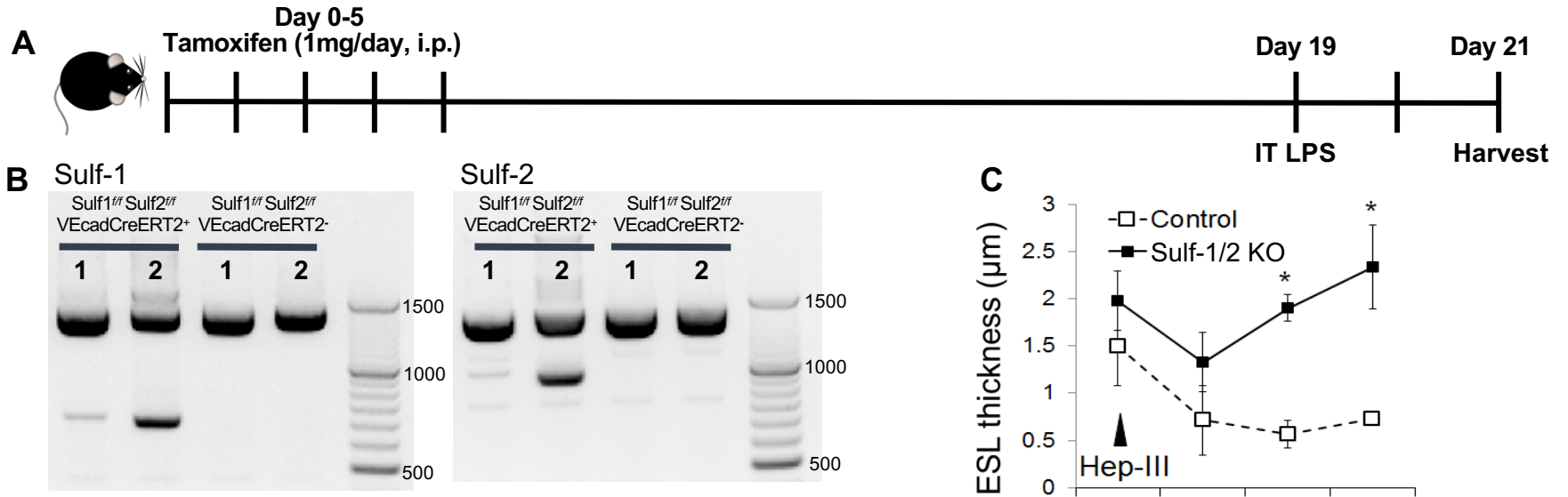


Figure 5 Loss of Sulf-1 is not sufficient to cause CARS in non-septic mice



1: FAC sorted non-endothelial cells (CD31⁻/CD144⁺); 2: FAC sorted endothelial cells (CD31⁺/CD144⁺)

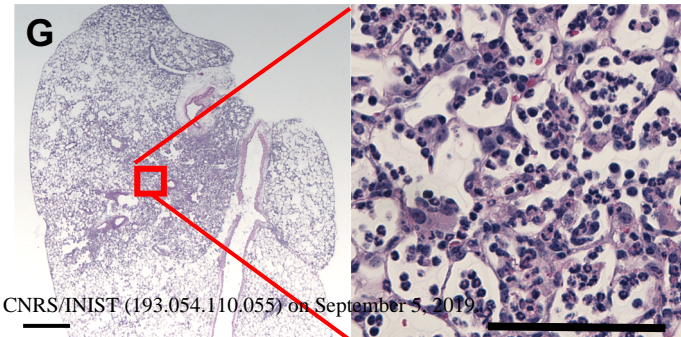
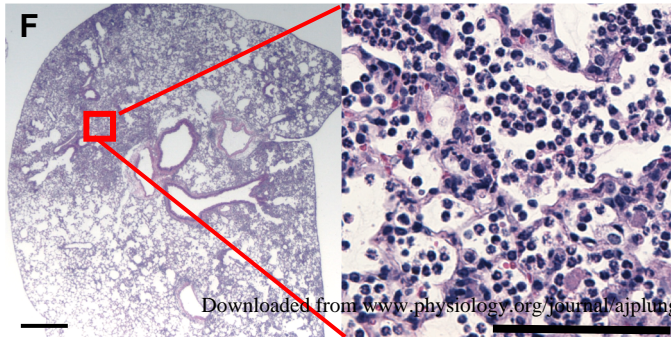
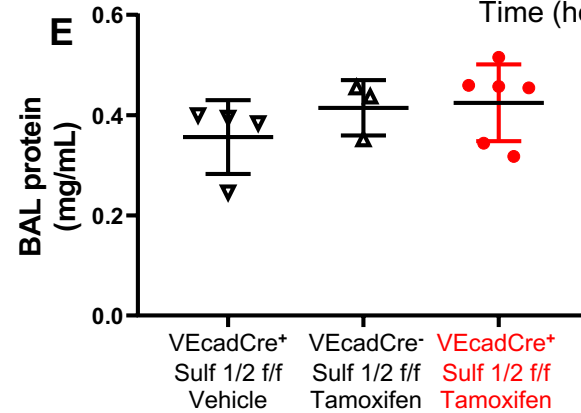
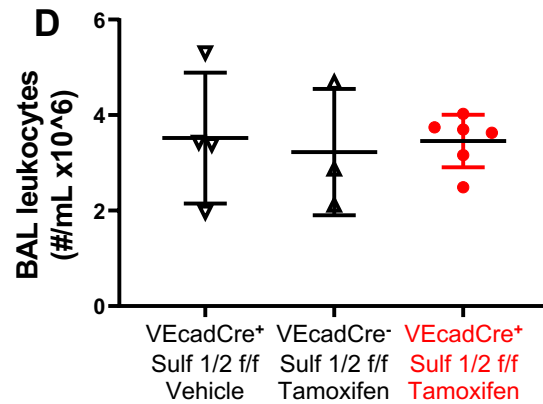


Figure 6 Knocking down Sulf-1 in pulmonary microvascular endothelial cells decreases ICAM-1 expression

